Stiff Coatings on Compliant Biofibers:

The Cuticle of *Mytilus californianus* Byssal Threads†,‡

Niels Holten-Andersen§,⊥, **Hua Zhao**‖,⊥, and **J. Herbert Waite***,§,‖

§Biomolecular Science & Engineering Graduate Program, University of California, Santa Barbara, California 93106

‖Marine Science Institute, University of California, Santa Barbara, California 93106

Abstract

For lasting holdfast attachment, the mussel *Mytilus californianus* coats its byssal threads with a protective cuticle 2-5 μm thick that is 4-6 times stiffer than the underlying collagen fibers. Although cuticle hardness (0.1 GPa) and stiffness (2 GPa) resemble those observed in related mussels, a more effective dispersion of microdamage enables *M. californianus* byssal threads to sustain strains to almost 120% before cuticle rupture occurs. Underlying factors for the superior damage tolerance of the byssal cuticle were explored in its microarchitecture and in the cuticular protein, mcfp-1. Cuticle microstructure was distinctly granular, with granule diameters (~200 nm) only a quarter of those in *M. galloprovincialis* cuticle, for example. Compared with homologous proteins in related mussel species, mcfp-1 from *M. californianus* had a similar mass (~92 kDa) and number of tandemly repeated decapeptides, and contained the same post-translational modifications, namely, *trans*-4-hydroxyproline, *trans*-2,3-*cis*-3,4-dihydroxyproline, and 3,4-dihydroxyphenylalanine (Dopa). The prominence of isoleucine in mcfp-1, however, distinguished it from homologues in other species. The complete protein sequence deduced from cDNAs for two related variants revealed a highly conserved consensus decapeptide PKISYPPTYK that is repeated 64 times and differs slightly from the consensus peptide (AKPSYPPTYK) of both *M. galloprovincialis* and *M. edulis* proteins.

Coatings, especially thin coatings, provide little in the way of mechanical support for bulk materials loaded in tension or compression. They can, however, make a substantial contribution to material durability, especially in abrasive, corrosive, desiccated, or hydrolytic environments (1). Specialized coatings are present on most exposed biological surfaces, including the waxy cuticles on plant leaves (2) and insect exoskeletons (3), the enamel on teeth (4), the periostracum on seashells (5), and the epidermis of skin (6). A cuticle ~5 μm thick coats all exposed surfaces of the byssus (7), a fibrous holdfast in marine mussels (Figure 1A) that provides tenacity against the lift and drag forces of waves. The byssal cuticle serves to protect against at least two forms of deterioration: microbial attack and abrasion by suspended sand particles (8,9).

Like other *Mytilus* species, *M. californianus* lives attached to rocks in the surf zone. However, the bigger waves and 10-fold higher wave impacts of the Californian surf (10), subject the California mussel byssus to significantly more deformation in tension and abrasion by suspended sand. Given that strains of 10-70% are common in byssal threads (11), a better

*To whom correspondence should be addressed. Tel: 805 893-2817. Fax: 805 893-7998. E-mail: waite@lifesci.ucsb.edu.
⊥These authors contributed equally to this work.

understanding of the adaptive mechanisms that exist in the cuticle for mitigating damage at high strains has fundamental scientific and technological value. Cuticles that rupture in strain quickly lose their ability to protect against deterioration. A recent comparison of the cuticles of mussel species from calm and agitated waters revealed that, although the two had similar stiffness and hardness properties, they exhibited unexpected differences in microarchitecture and nanomechanics (12,13). The cuticle from the calm water mussel was smooth and homogeneous, whereas in mussel byssus from agitated habitats, it resembled sliced salami, i.e., with spherical ~1 μm granules dispersed in a continuous matrix. The granular cuticle provided superior protection for the underlying collagen fibers by combining a hardness (4 to 6 times greater than that of the fibrous core) with damage management apparent as microtears dispersed throughout the cuticle during deformation at strains up to 40%. Microtears are preferable to larger catastrophic cuticle ruptures since the latter tend to be irreversible and expose the underlying collagens directly to abrasion as well as to microbial collagenases.

The byssal cuticles of mytilids contain metal ions (14,15), highly repetitive proteins known as type-1 mussel foot proteins (mfp-1) (14,16), and possibly fatty acids (17). Mefp-1[1] from *M. edulis*, for example, consists of 75 tandem repeats of a decapeptide sequence AKP*SY*P*P-*TY*K (18,19) in which the * residues are hydroxylated as follows: P* *trans*-4-hydroxyproline (Hyp), Y* 3,4-dihydroxyphenyl-L-alanine (Dopa), and P* *trans*-2,3-*cis*-3,4-dihydroxyproline (20,21). The related mgfp-1 from *M. galloprovincialis* has the same tandem decapeptide repeats but a distinct N-terminal domain (14,22). The relationship between sequence and cuticle microstructure remains unexplored.

The hardness and damage mitigation associated with a granular microarchitecture in the byssal cuticle prompted our interest in the byssus of the California mussel, *M. californianus*, the undisputed champion of tenacity in the high surf-zone (23). This study suggests that subtle structural and biochemical differences in the byssal cuticles of *M. galloprovincialis* and *M. californianus* can translate into substantial gains for cuticle durability. The damage tolerance

---

[1]Abbreviations:

mcfp-1
> *Mytilus californianus* foot protein 1

mefp-1
> *Mytilus edulis* foot protein 1

mgfp-1
> *Mytilus galloprovincialis* foot protein 1

pcfp-1
> Perna canaliculus foot protein 1

Dopa
> 3, 4-dihydroxyphenylalanine

MALDI-TOF
> matrix assisted laser desorption and ionization with time-of-flight

PCA
> perchloric acid

PAGE
> polyacrylamide gel electrophoresis

RT-PCR
> reverse transcriptase-polymerase chain reaction

RACE
> rapid amplification of cDNA ends

of the California mussel cuticle is clearly superior to that of other mussel species and, for that matter, to any available synthetic coating for compliant materials.

MATERIALS AND METHODS

Microscopical Analysis: M. californianus

Conrad specimens were collected from Goleta Pier at Santa Barbara, CA and allowed to reattach in an open circulating seawater tank at about 15 °C. For scanning electron microscopy (SEM), mussel threads were mounted on conductive carbon tabs on SEM posts (Ted Pella, Redding, CA), sputter-coated using a Desk-II coater equipped with a gold/palladium target (Moorestown, NJ), and imaged in a scanning electron microscope (Vega Ts 5130 mm, Tescan, Czech Republic). For Transmission electron microscopy (TEM), threads were stained with osmium tetroxide, fixed in glutaraldehyde/paraformaldehyde, embedded in Spurrs resin (Polysciences, Inc., Warrington, PA) and microtomed (Leica EM UC6, Leica Mikrosysteme GmbH, Vienna, Austria) to produce thin sections of 80 nm, following standard protocols. Micrographs were obtained using a JEOL 123 transmission electron microscope (Pleasanton, CA) operated at 80 kV. The size-distributions of the granular inclusions in the two different cuticles were determined from transmission electron micrographs.

Mechanical Properties

To compare the effects of stretching on the two different cuticles, the ends of the threads were embedded in pyramid shaped blocks of Epofix (Electron Microscopy Sciences, Hatfield, PA) to provide a nonslip grip. One end of a thread was then securely clamped to the side of a Petri dish mounted on an Eclipse ME600 light-microscope (Nikon Instruments Inc., Melville, NY), after which the whole thread was submerged in milliQ water. Using a micromanipulator (Narishige CO., Ltd., Tokyo, Japan) attached to the microscope stage, each thread was subsequently pulled under water in 10% increments of its initial length. This setup allowed direct observation of macroscopic fracture development in the cuticle as a function of strain. Counting the total number of observed fractures accumulated before final thread rupture as 100%, the evolution of macroscopic damage of the cuticle of each fiber was normalized. After pulling multiple threads ($N = 12$), an average macroscopic fracture number density was then calculated at each strain increment. Some threads were dried in the strained state followed by freeze-drying overnight. Desiccation locks the strain in stretched threads to be imaged by scanning electron microscopy. Unstretched control threads taken through the same drying procedure were also examined.

To measure the local effects of strain in the granular coating of *M. californianus*, fibers stretched to 70% were dried alongside unstretched fibers and embedded in Epofix. Longitudinal cross-sections of the distal portions of the threads were prepared with a microtome. The local damage in the granular coating was detected by AFM imaging in air (MFP-3D-BIO AFM, Asylum Research, Santa Barbara, CA).

Young's moduli and hardness values for the cuticle and the thread interior were obtained for both species by nanoindentation. Tests were performed on microtomed surfaces of transverse cross-sections of threads embedded in Epofix, with test specimens submerged in milliQ water. Indentation tests were performed using a TriboIndenter (Hysitron, Minneapolis, MN) with a cube corner diamond tip. The tip area function was established from a PMMA standard. All load-displacement curves were analyzed using the method described by Oliver and Pharr (24). Images of the sample surfaces were obtained by scanning probe microscopy (SPM) immediately before and after each indentation to ensure correct placement of indents. All indentations were carried out in the open loop feedback mode under loading rate control. The loading and unloading rates were 100 μN/s; the peak load was approximately 1000 μN. Once

at the peak, the load was held fixed for a period of 30 s, for the purpose of eliminating creep effects.

Protein Extraction and Purification

In preparation for an extraction, mussels were killed by severing the adductor muscles, following which the feet were carefully dissected and either used directly or stored at -80 °C until use. About 10 g of frozen mussel feet were partially thawed, sliced into small pieces with a clean single-edge razor blade, and homogenized on ice in 50 mL of 5% acetic acid (v/v) with protease inhibitors (10 mg/L pepstatin and 10 mg/L leupeptin) using a frosted-glass Kontes tissue grinder. The homogenate was centrifuged at 20,000g for 40 min in a refrigerated Sorval 5B centrifuge, and the supernatant (about 45 mL) was collected and kept in an ice-cold bath. Chilled 70% perchloric acid (PCA) was added dropwise to give a final PCA concentration of 1.4%. The mixture was stirred on ice for 30 min and centrifuged at 20,000g for 30 min. The pellet was discarded, while the supernatant was dialyzed overnight at 4 °C against 4 L of 5% acetic acid using dialysis tubing with a molecular weight cutoff of 1,000. The dialysates were freeze-dried and redissolved in a small volume of 5% acetic acid. This concentrated crude extract of Mcfp-1 was subjected to further purification. Pure mcfp-1 was achieved by gel filtration chromatography with a Shodex KW-803 column (5 μm, 8×300 mm). The column was equilibrated and eluted with 5% acetic acid with 0.2% TFA at a flow rate of 0.2 mL/min. A maximum 200 μL of crude concentrate was loaded onto the Shodex KW-803 column in each run according to Ohkawa et al. (25). The elutants were monitored at 280 nm, and mcfp-1 containing fractions were pooled and further polished by reverse-phase C8 HPLC.

Electrophoresis

Routine electrophoresis was performed on polyacrylamide gels (7.5% acrylamide and 0.2% *N,N*'-methylenebisacrylamide) containing 5% acetic acid with 8 M urea. The advantage of this type of polyacrylamide gel electrophoresis (PAGE) for the analysis of Dopa-containing proteins is that it can be processed for protein or Dopa staining with equal facility. Proteins were stained with Serva Blue R (Serva Fine Chemicals, Westbury, NY), whereas Dopa was stained with either the Arnow reagent (26) or nitro blue tetrazolium redox cycling (27).

Amino Acid Analysis and Protein Sequencing

Purified mcfp-1 was hydrolyzed in 6 M HCl with 5% phenol in vacuo at 110 °C for 24 h. The hydrolysate was flash evaporated at 50 °C under vacuum and washed to dryness with small volume Milli Q-water followed by methanol. Amino acid analysis was performed according to conditions described earlier (28) with a Beckman System 6300 Auto Analyzer. Amino acid sequence of the intact Mcfp-1 was determined by automated Edman degradation on a microsequencer (Porton Instruments, Model 2090, Tarzana, CA) calibrated with phenylthiohydantoin (PTH) derivatives of the amino acid standards including Dopa *trans*-4-hydroxyproline and *trans*-2,3-*cis*-3,4-dihydroxyproline (21,28).

Molecular Cloning

Total RNA was extracted from the phenol and accessory glands in a single *M. californianus* foot using an RNase Plant Mini Kit from Qiagen (Valencia, CA, USA). Qiagen's protocols were followed to the letter after disrupting foot tissue under liquid nitrogen with a mortar and pestle. A cDNA library was constructed using mRNA purified from total RNA using the CloneMiner cDNA Library Construction Kit from Invitrogen. In addition, first strand cDNA was synthesized from total RNA using Superscript II reverse transcriptase with an adapter primer, 5′-GGC CAC GCG TCG ACT AGT ACT (T)$_{16}$-3′ (Invitrogen). The product of the RT reaction was used as an alternative template source for PCR.

The partial mcfp-1 sequence has been available since 1986 (19,29), but the cDNA sequence is limited to mfp-1 from *M. edulis* and *M. galloprovincialis*. On the basis of the high sequence identity of decapeptide repeats of all known *Mytilus* mfp-1s, some primers were designed from Mgfp-1 cDNA (accession number: Q27409) to amplify partial sequences of mcfp-1 cDNA from both the cDNA library and the reverse transcribed template. Two primers, *for-1* (5′-TCT AAG GCA AGT TAT CCC CCT TCT TAT-3′ (codes for SKASYPPSY) and an abridged *universal* amplification *primer* (antisense 5′-GGC CAC GCG TCG ACT AGT AC-3′) from Invitrogen, were used to amplify the carboxyl-terminal of mcfp-1 with 3′-untranslated region from the RT template. Two additional primers, *for-2* (5′-ATG GAG GGA ATC AAA TTA AAT CTG TGC-3′; codes for MEGIKLNCL) and *rev-2* (5′-GGT TTA TAT GTT GGA GGA TAA GTT TTC T-3′; codes for KTYPPTYKP), were used to amplify the amino-terminal of mcfp-1 from the cDNA library. For cloning and amplifying the middle portion of mcfp-1, *for-3* (5′-CA GTT TAT AAA CAT AAG ATA ACT AAT C C-3′; Codes for VYKHKITNP) and *rev-3* (5′-GGT TGA TAA GAA GGG GGA TAA CTT GCC T-3′; codes for ASYPPSYQP) were designed according to the known amino- and carboxyl-terminal sequence. The complete sequence of Mcfp-1 was then achieved by mapping overlaps in the partial cDNA clones.

PCRs were carried out in 25 μL of 1 × buffer B (Fisher) and 5 pmol of each primer, 5 μmol of each dNTP, 1 μL of first strand reaction, and 2.5 units of Taq DNA polymerase (Fisher) for 35 cycles on a Robocycler (Stratagene). Each cycle consisted of 30 s at 94°, 30 s at 52°, and 1 min at 72°, with a final extension of 15 min. The PCR products were subjected to 1% agarose gel electrophoresis, purified, and cloned into a PCR TA vector (TOPO TA Cloning Kit, Invitrogen) and transformed into competent Top10 cells for amplification, purification, and sequencing.

To obtain full sequence to the 5′-end, a GeneRacer kit from Invitrogen based on 5′ RACE was applied to full-length transcripts. PCR was performed with a gene specific primer (antisense 5′-GAT ATA TAT GAT GTT GGA ATC TTA TTC AT-3′; MNKIPTSYIS), which reverse primes the cDNA corresponding to the N-terminus of mcfp-1 with a GeneRacer 5′ primer from Invitrogen (sense 5′-CGA CTG GAG CAC GAG GAC ACT GA-3′).

Mass Spectrometry

The mass of Mcfp-1 was determined by matrix-assisted laser desorption and ionization with time-of-flight (MALDI-TOF) using a PerSeptive- Biosystems Voyager DE model (AB Biosystems, Foster City, CA) in the positive ion mode with delayed extraction. The MALDI matrix was prepared by dissolving sinapinic acid (10 mg/ml) in 30 vol % acetonitrile. Purified Mcfp-1 was dissolved in this matrix solution to give a final concentration between 1 and 10 pmol/μL. About 1 μL of this solution was spotted to the target plate and allowed to vacuum-dry. The sample spots were irradiated using a N_2 laser with a wavelength of 337 nm, pulse width of 8 ns, and frequency of 5 Hz. MALDI ionization generates monoprotonated, doubly charged, and triprotonated ions for the mcfp-1 protein, which were accelerated using either 20 or 25 kV accelerating voltage. For comparison, mgfp-1, purified according to Sun (14), was also subjected to MALDI-TOF mass spectrometry (Supporting Information). Bovine serum albumin was used as molecular mass calibrant having 66,430 and 33,215 as the mono- and diprotonated ions, respectively.

Chemical Analyses

The discrepancy between the virtual masses calculated for the cDNA-deduced protein sequences of mcfp-1 variants and actual masses observed by MALDI TOF mass spectrometry prompted a search for covalent modifications. Between 10-20 μg purified mcfp-1 was used in each of the following assays: neutral sugars (30), amino sugars (31), and phosphoserine and phosphothreonine (32).

RESULTS

Cuticle Microstructure

Microscopic inspection of byssal threads from *M. californianus* revealed a granular cuticle about 2-5 μm thick covering the exterior of the threads (see Figure 1b). As in *M. galloprovincialis*, the California mussel cuticle resembles a composite with granular inclusions uniformly distributed within a continuous matrix (see Figure 1c). Although the granules of the *M. californianus* cuticle appear more homogeneous than those of *M. galloprovincialis*, higher magnification images reveal a similar convoluted structure (33). The granule dimensions for *M. californianus*, however, are significantly smaller with an average diameter of 200 ± 80 nm ($N = 264$) compared with 750 ± 200 nm ($N = 207$) for *M. galloprovincialis* (Figure 1d). In both cases, the granules comprise about 50% of the cuticle volume. On the basis of the similar volume fractions, the smaller granule diameter in the cuticle of *M. californianus* significantly increases the granule-matrix interfacial area by a factor of 4.

Biomechanical Properties of the Thread

To explore the effect of strain on cuticular structure, we used SEM and AFM to scrutinize cuticles of stretched and relaxed byssal threads. Two types of cuticle damage became evident with increasing strain: macrotears (>10 μm) and microtears (1-10 μm) (Figure 2b). In *M. californianus*, macrotears did not develop below 70% and occasionally required >100% strain, whereas in *M. galloprovincialis*, macrotear onset was at 40% strain. Macrotears, however, were preceded by microtears, which appear as small, localized gaps between the matrix and granules. That cuticles of both species sustain microtear damage was determined by analyzing all AFM images of threads at 50% strain for the % of total cuticle area covered by microtears. In *M. galloprovincialis*, microtears represent about 1% of the cuticle (variance ± 0.00022, $n = 9$); in contrast, in *M. californianus*, microtears covered 3.8% of the cuticle (variance ± 0.00161, $n = 6$). These differences are significant (>99% by a paired *t*-test) and suggest that increased strain tolerance in the *M. californianus* cuticle depends not on microtear suppression but rather on an effective suppression of microtear merger into macrotears. Microtears were not observed in the sectioned unstrained cuticle. That microtears are created when the microtome knife hits a strain-hardened granule during sectioning remains possible but granule-matrix differences in hardness and stiffness were not evident in our indentation analysis of cuticle.

Remarkably, the significant increase in *M. californianus* cuticle strain capacity does not compromise its hardness. Nanoindentation tests revealed that the Young's modulus, *E*, and hardness, *H*, of hydrated thread cuticles of the two mussel species are similar (Figure 2C) and comparable to those of structural engineering polymers. Both byssal cuticles have a stiffness (*E*) and hardness (*H*) of about 1.7 and 0.1 GPa, respectively, and are between 4-6 times greater than the *E* and *H* of the core collagens.

Protein Purification

A partial characterization of mcfp-1 was reported earlier (29). Here, mcfp-1 quality and yield were improved by the extraction of foot tissue with perchloric acid (34) and the use of both molecular filtration and reverse phase chromatography (Supporting Information). Peak fractions obtained by reverse-phase C8 HPLC were subjected to MALDI-TOF mass spectrometry, amino acid sequencing, and amino acid composition analysis. Mass spectrometry revealed two variants by pairs of singly, doubly, and triply protonated ions at *m/z* 92,177/82,424, 46,108/41,234, and 30,735/27,512, respectively. N-terminal sequencing of the mcfp-1 gave a single sequence, FIHNAY*GSAY*, where Y* denotes Dopa. Amino acid analysis of pure mcfp-1 revealed a strong compositional bias (Table 1). Hyp, Lys, Dopa, Thr, and Ser dominate the composition; when combined, these tally to 66 mol %. *trans*-4-hydroxyproline *(*Hyp) and *trans*-2,3-*cis*-3,4-dihydroxyproline (di-Hyp) were detected at 18.2

mol % and 5.9 mol %, respectively. Trp and cystine (Cys/2) were not detected, while Arg was observed at about 1.0 mol%.

Molecular Cloning

Using a routine cloning strategy with nondegenerate primers from *M. galloprovincialis* mgfp-1 cDNA (EMBL-EBI D63778), the complete sequence of two mcfp-1 variants was deduced from overlapping cDNA clones (Figure 4 and Supporting Information). The signal peptide cleavage site predicted by SIGNALP (EXPASY) is between G-24 and F-25 and is consistent with the sequenced N-terminus of mcfp-1. The consensus tandem-repeat motif of mcfp-1 is PKISYPPTYK, which occurs 64 times in variant 1 (57 times in variant 2) and extends to the C-terminus. The 5th, 6th, and 10th positions are nearly 100% conserved. Position #1 of the decapeptide is dominated by Pro (62%) and sometimes substituted by Arg, Ala, and Ser. Position #3 is dominated by Ile (33%) or Pro (30%) when substituted. The calculated pI of 10.34 is slightly higher than that in the mfp-1s of *M. edulis* and *M. galloprovincialis* (Figure 5). Except for a gap of seven decapeptide repeats between #224-294, variant 2 has the same sequence as variant 1.

The discrepancy between the calculated masses of the cDNA-deduced sequence of variants A and B (82.4 kDa, and 75.4 kDa) and the actual masses as measured by mass spectrometry (92,177 and 82,424 Da) (Figure 5) appears due to post-translational modifications. A rough calculation indicates that if all the Tyr and Pro in variant 1 were hydroxylated to Dopa and the mono- and dihydroxylated forms of Pro, respectively, then the unmodified mass would be increased by 6 kDa to 88.4 kDa. This leaves about 3.8 kDa unaccounted for. Mcfp-1 contains no detectable glycosylation by neutral or amino sugars and no phosphorylation based on methods described in Materials and Methods (results not shown). Acylation by fatty acids is not supported by extensive mass analysis of tryptic peptides ((28) results not shown). Thus, the modifications responsible for the remaining mass discrepancy remain unknown.

DISCUSSION

Stiff coatings covering more compliant cores are risky constructs, and the degree of risk increases with strain as illustrated by the following example: A rubber band dipped briefly into molten paraffin acquires a waxy coating that is several times harder and stiffer than the rubber at room temperature. After a 10% extension, the paraffin coating exhibits a network of cracks; at 50%, it disintegrates by delaminating from the rubber. Studies by Holten-Andersen et al. (12) showed that byssal cuticles of mussels from quiescent habitats fail catastrophically at low strains, like the paraffin on rubber. In contrast, more exposed mussels, such as *M. galloprovincialis*, have evolved composite cuticles that delay catastrophic rupture by distributing failure throughout the cuticle in the form of microtears between the matrix and granular filler (12).

In the most exposed mussel, *M. californianus*, thread strain routinely exceeds 70%, but catastrophic rupture of the byssal cuticle requires a thread strain >100%. Microtears were abundantly apparent below that strain. The superior range of damage distribution in the byssal cuticle suggests improved microarchitecture, matrix biochemistry, or both. With respect to microarchitecture, the cuticle of *M. californianus* resembles that of *M. galloprovincialis* in three respects: thickness, granule shape, and volume fraction of granules. The *M. californianus* granule diameters, however, are a quarter of those found in *M. galloprovincialis* cuticles, which gives the former four times more surface area per unit volume for interaction with the matrix.

Does fracture energy in composites scale with the interfacial area between the matrix and filler? Apparently, there is no simple answer to this. For the highest fracture energy in epoxies filled

with silica spheres, the optimal sphere diameter was not the smallest tested (35). Other critical contingencies, such as filler volume fraction, strong or weak interfacial adhesion, as well as filler and matrix type, significantly influence the relationship. The dependence of byssal cuticle on microstructure thus awaits a better characterization of the matrix and granule properties.

Mussel fp-1 is crucial to the relationship between matrix and granules since localization mfp-1 autofluorescence suggests it is present in both (15). The primary sequence of mcfp-1 is highly homologous (>80%) with that of mgfp-1 and mefp-1 (N.B. the *M. edulis* cuticle is granular and virtually indistinguishable from the *M. galloprovincialis* cuticle in every detail). More than three-quarters of the protein consists of a tandemly repeated decapeptide (Figure 5 consensus) in which Lys, Dopa, and Pro/Hyp are mostly or entirely conserved. Indeed, only positions #1 and #3 show significant variation, i.e., PKISYPPTYK (Mc) vs AKPSYPPTYK (Mg). Apart from switching the Pro from one side of Lys-2 to the other, introduction of highly hydrophobic Ile into the decapeptide sequence is noteworthy, given that after post-translational modification, all the other residues become quite polar. The cDNA-deduced sequence of a homologue from an Asian species, *M. coruscus*, shows a similar placement of Ile in the consensus sequence as in mcfp-1, but no other details are known about this protein (36). An intriguing difference between mcfp-1 (variant 1) and the mfp-1s of other mussels is a mass discrepancy of about 4 kDa between the virtual mass (cDNA-deduced protein sequence) and the observed mass after adjusting for all known hydroxylations. Mefp-1 and mgfp-1 show no such discrepancy; for example, adding ~6 kDa for all known hydroxylations of Pro and Tyr to 102 kDa (the virtual mass of mefp-1) results in 108 kDa, which agrees with the observed mass (Figure 5).

Mcfp-1 is the only known protein in the byssal cuticle, but it is not the only constituent. Metal ions, notably calcium and iron, are present at up to 1% by weight (14,15). The contribution of dopa-metal coordination complexes to a material's ability to self-mend after damage has been discussed previously (37,38). Byssal threads are also reported to be about 8% fatty acids by dry weight (17), and fatty acid enrichment in the byssal cuticle is consistent with the strong osmiophilicity of the cuticle matrix (e.g., Figure 1B) (7,9). On the basis of intrinsic dopa fluorescence in situ, mfp-1s appear uniformly distributed in both the matrix and granular phases of the cuticle (15); this, however, would not prevent different variants from preferring one particular phase or another. If the variants are uniformly distributed, then the main biochemical difference between the granular and matrix phases may be related to how other components such as fatty acids distribute themselves. To date, no detectable differences in mechanics or chemistry between the granular and matrix phases have emerged.

Byssal cuticles are compelling paradigms as wear and damage resistant coatings for compliant materials. Deeper insights necessary for understanding how they work will require high-resolution spatial analysis of cuticle chemistry and mechanics.

Supplementary Material

Refer to Web version on PubMed Central for supplementary material.

ACKNOWLEDGMENT

REFERENCES

1. Schoff CK. Organic coatings: the paradoxical materials. Prog. Org. Coatings 2005;52:21–27.

2. Bargel H, Koch K, Cerman Z, Neinhuis C. Structure-function relationships of the plant cuticle and cuticular waxes - a smart material? Funct. Plant Biol 2006;33:893–910.

3. Neville, AC. Biology of Fibrous Composites: Development beyond the Cell Membrane. Cambridge University Press; Cambridge, U.K.: 1993.

4. Popowics TE, Rensberger JM, Herring SW. Enamel microstructure and microstrain in human and pig molar cusps. Arch. Oral. Biol 2004;49:595–605. [PubMed: 15196977]

5. Waite JH, Andersen SO. 3,4-Dihydroxyphenylalanine and the sclerotization of periostracum in *Mytilus edulis*. Biol. Bull 1980;158:164–173.

6. Wolff-Schreiner EC. The ultrastructural cytochemistry of the epidermis. Int. J. Dermatol 1977;16:77–102. [PubMed: 321372]

7. Vitellaro Zuccarello L. Ultrastructural and cytochemical study on the enzyme gland of the foot of a mollusk. Tissue Cell 1981;13:701–713. [PubMed: 6800062]

8. Dreisbach JH, Merkel JR. Induction of collagenase production in *Vibrio* B-30. J. Bacteriol 1978;135:521–527. [PubMed: 210154]

9. Zardi GI, Nicastro KR, McQuaid CD, Erlandsson J. Sand and wave induced mortality in invasive *(Mytilus galloprovincialis)* and indigenous *(Perna perna)* mussels. Mar. Biol 2008;153:853–858.

10. Harger JRE. The effect of wave impact on some aspects of the biology of sea mussels. Veliger 1970;12:401–414.

11. Carrington E, Gosline JM. Mechanical design of mussel byssus: Load cycle and strain dependence. Am. Malacol. Bull 2004;18:135–142.

12. Holten-Andersen N, Fantner GE, Hohlbauch S, Waite JH, Zok FW. Protective coatings on extensible biofibers. Nat. Mater 2007;6:669–672. [PubMed: 17618290]

13. Holten-Andersen N, Slack N, Zok F, Waite JH. Nano-mechanical Investigation of the byssal cuticle, a protective coating of a bio-elastomer. Mater. Res. Soc. Symp. Proc 2005;841:R3.7.1–Y3.7.1.

14. Sun CJ, Waite JH. Mapping chemical gradients within and along a fibrous structural tissue: Mussel byssal threads. J. Biol. Chem 2005;280:39332–39336. [PubMed: 16166079]

15. Holten-Andersen N, Mates T, Toprak M, Stucky GD, Zok FW, Waite JH. Metals and the integrity of a biological coating: the cuticle of mussel byssus. Langmuir. 2008[Online early access], DOI: 10.1021/la8027012, published online Oct 11, 2008

16. Benedict CV, Waite JH. Location and analysis of byssal structural proteins of *Mytilus edulis*. J. Morphol 1986;189:261–270. [PubMed: 3772980]

17. Cook, M. Adhesion in Biological Systems. Manly, RS., editor. Academic Press; New York: 1970. p. 139-150.

18. Filpula DR, Lee SM, Link RP, Strausberg SL, Strausberg RL. Structural and functional repetition in a marine mussel adhesive protein. Biotechnol. Prog 1990;6:171–177. [PubMed: 1367451]

19. Laursen, R. Reflections on the Structure of Mussel Adhesive Proteins. In: Case, ST., editor. Results and Problems in Cell Differentiation 19 Biopolymers. Springer-Verlag; Berlin, Germany: 1992. p. 55-74.

20. Waite JH. Evidence for a repeating 3, 4-dihydroxyphenylalanine and hydroxyproline containing decapeptide in the adhesive protein of the mussel *Mytilus edulis*. J. Biol. Chem 1983;258:2911–2915. [PubMed: 6298211]

21. Taylor SW, Waite JH, Ross MM, Shabanowitz J, Hunt DF. trans-2,3- cis- 3,4-Dihydroxyproline in the tandemly repeated consensus decapeptides of an adhesive protein from *Mytilus edulis*. J. Am. Chem. Soc 1994;116:10803–10804.

22. Inoue K, Odo S. The adhesive protein cDNA of *Mytilus galloprovincialis* encodes decapeptide repeats and no hexapeptide motif. Bio. Bull 1994;186:349–355. [PubMed: 8043658]

23. Bell EC, Gosline JM. Mechanical design of mussel byssus: Material yield enhances attachment strength. J. Exp. Biol 1996;199:1005–1017. [PubMed: 9318809]

24. Oliver WC, Pharr GM. An improved technique for determining hardness and elastic modulus using load and displacement sensing indention experiment. J. Mat. Res 1992;7:1564–1583.

25. Ohkawa K, Nishida A, Yamamoto H, Waite JH. A glycosylated precursor protein from the green mussel *Perna viridis* with modified Dopa side-chains. Biofouling 2004;20:101–105. [PubMed: 15203964]

26. Waite JH, Benedict CV. Assay of DOPA in invertebrate structural proteins. Methods Enzymol 1984;107:397–413. [PubMed: 6438444]

27. Paz M, Flückinger R, Boak A, Kagan HM, Gallop PM. Specific detection of quinoproteins by redox-cycling staining. J. Biol. Chem 1991;266:689–692. [PubMed: 1702437]

28. Waite JH. Detection of peptidyl-DOPA by amino acid analysis and microsequencing techniques. Anal. Biochem 1991;192:429–433. [PubMed: 1903612]

29. Waite JH. Mussel glue from *Mytilus californianus* Conrad: A comparative study. J. Comp. Physiol 1986;156B:491–496.

30. Dubois M, Gilles KA, Hamilton JK, Rebers PA, Smith F. Colorimetric method for determination of sugars and related substances. Anal. Chem 1956;28:350–356.

31. Miserez A, Schneberk T, Sun CJ, Zok FW, Waite JH. The transition from stiff to compliant materials in squid beak. Science 2008;319:1816–1819. [PubMed: 18369144]

32. Martenson TM. Chemical properties, isolation, and analysis of O-phosphates in proteins. Methods Enzymol 1984;107B:3–22.

33. Tamarin A, Keller PJ. An ultrastructural study of the byssal thread forming system in *Mytilus*. J. Ultrastr. Res 1972;40:401–416.

34. Zhao H, Waite JH. Coating Proteins: Structure and Cross-linking in Fp-1 from the green shell mussel *Perna canaliculus*. Biochemistry 2005;44:15915–15923. [PubMed: 16313194]

35. Kitey R, Tippur HV. Role of particle size and filler-matrix adhesion on dynamic fracture of glass-filled epoxy. I. Macromeasurements. Acta Mater 2005;53:1153–1165.

36. Inoue K, Takeuchi Y, Takeyama S, Yamaha E, Yamazaki F, Odo S, Harayama S. Adhesive protein cDNA sequence of the mussel *Mytilus coruscus* and its evolutionary implications. J. Mol. Evol 1996;43:348–356. [PubMed: 8798340]

37. Lee H, Scherer NF, Messersmith PB. Single molecule mechanics of mussel adhesion. Proc. Natl. Acad. Sci. U.S.A 2006;103:12999–13003. [PubMed: 16920796]

38. Holten-Andersen N, Waite JH. Mussel designed protective coatings for compliant substrates. J. Dent. Res 2008;87:701–709. [PubMed: 18650539]

39. Taylor SW, Chase DB, Emptage MH, Nelson MJ, Waite JH. Ferric iron complexes of a Dopa-containing adhesive protein from *Mytilus edulis*. Inorg. Chem 1996;35:7572–7577.
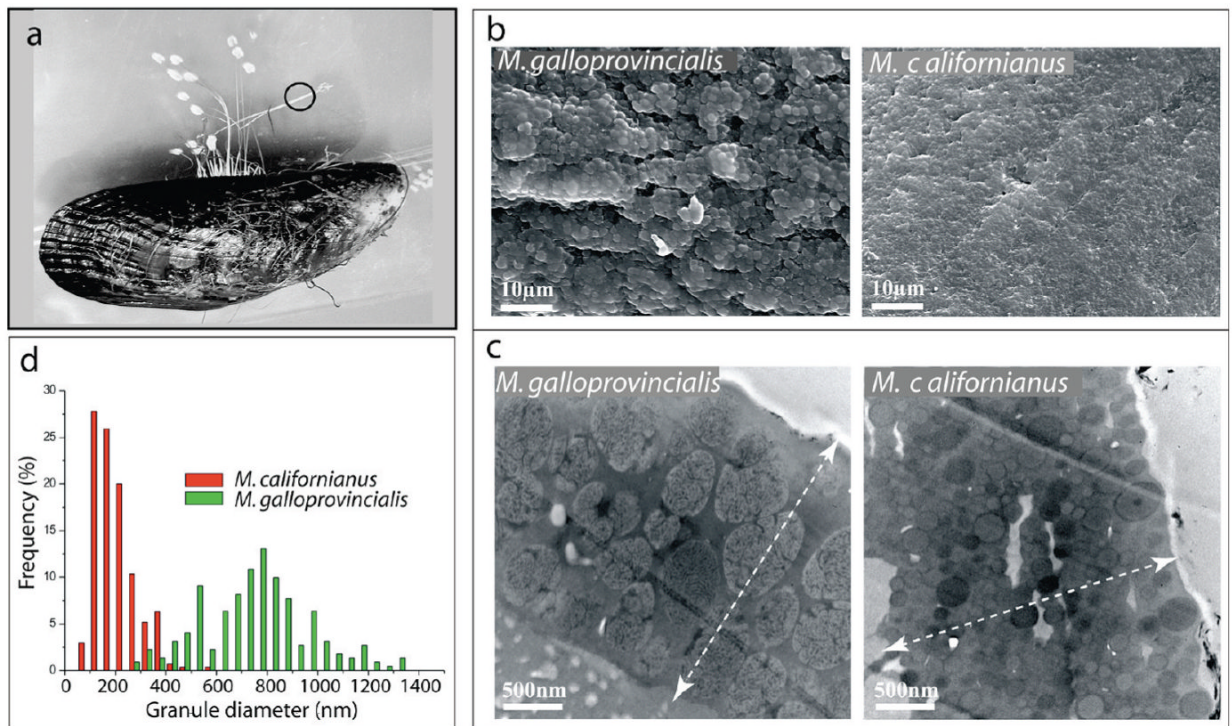
NIH-PA Author Manuscript

NIH-PA Author Manuscript

NIH-PA Author Manuscript

Figure 1.
Microstructure of byssal cuticles. (A) California mussel (length ~5 cm) showing byssal threads and distal thread portion (circle). (B) SEM of the granular cuticles on the distal portion of threads from *M. galloprovincialis* and *M. californianus* illustrating the micro- and nanoscale composite structure. (C) TEM of transverse sections of byssal thread cuticles revealing micron- and submicron-sized granules of *M. galloprovincialis* and *M. californianus*. (D) Size-distribution histogram of granules in the two cuticles.
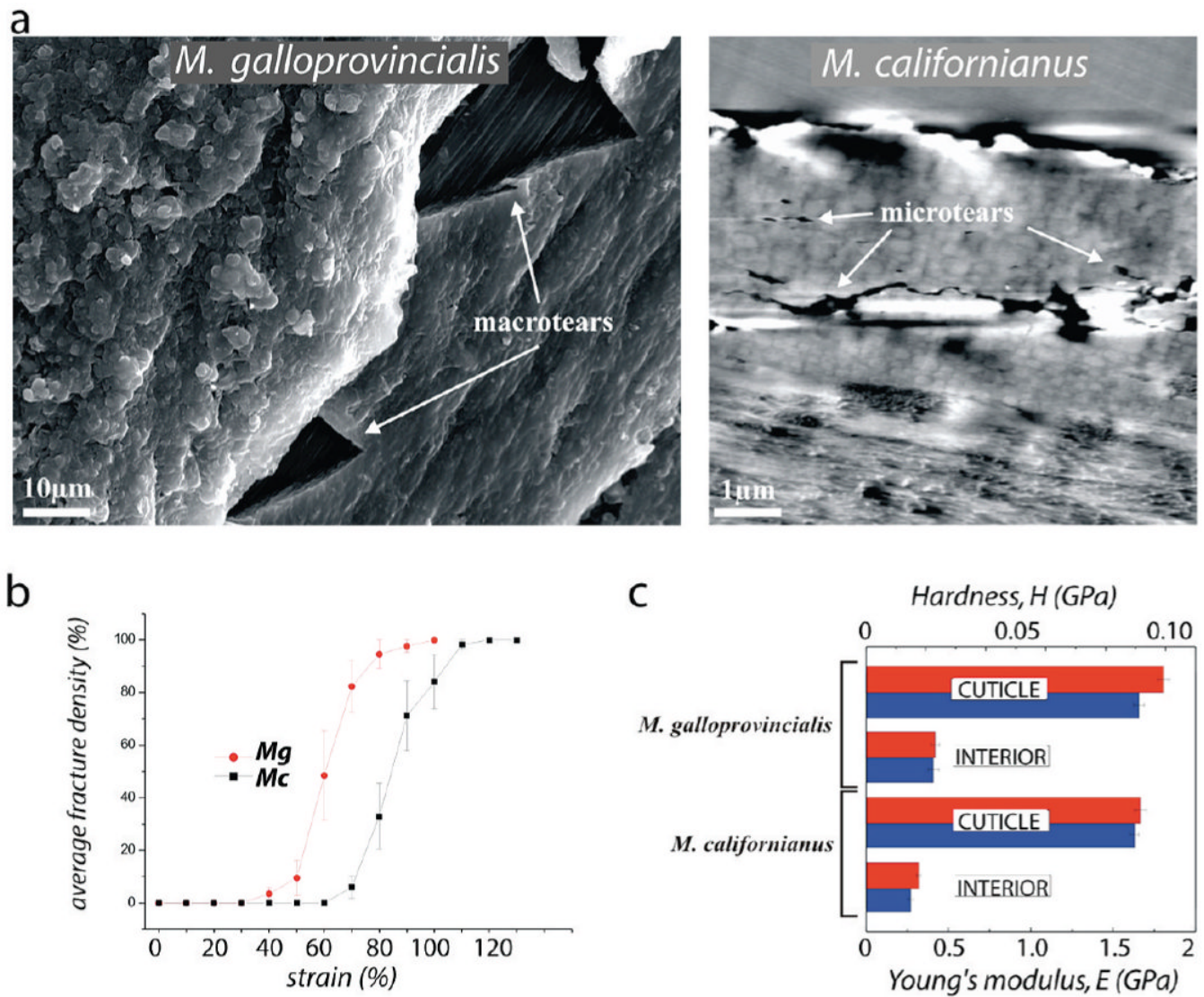
Figure 2.
Strain tolerance of coatings. (A) At 70% strain, *M. galloprovincialis* byssal cuticle (left) fails catastrophically, whereas the cuticle of *M. californianus* (right) exhibits only microtears. (B) Cuticle macrotear formation during thread extension can be monitored by microscopic inspection. *M. californianus* cuticle has a higher strain capacity compared to that of *M. galloprovincialis* as demonstrated by its lower tear tendency or fracture density at any given strain (100% average fracture density represents whole thread failure). (C) Nanoindentational hardness and modulus of hydrated thread cuticle and interior of both mussel species ($N = 13$; brackets are standard deviations).
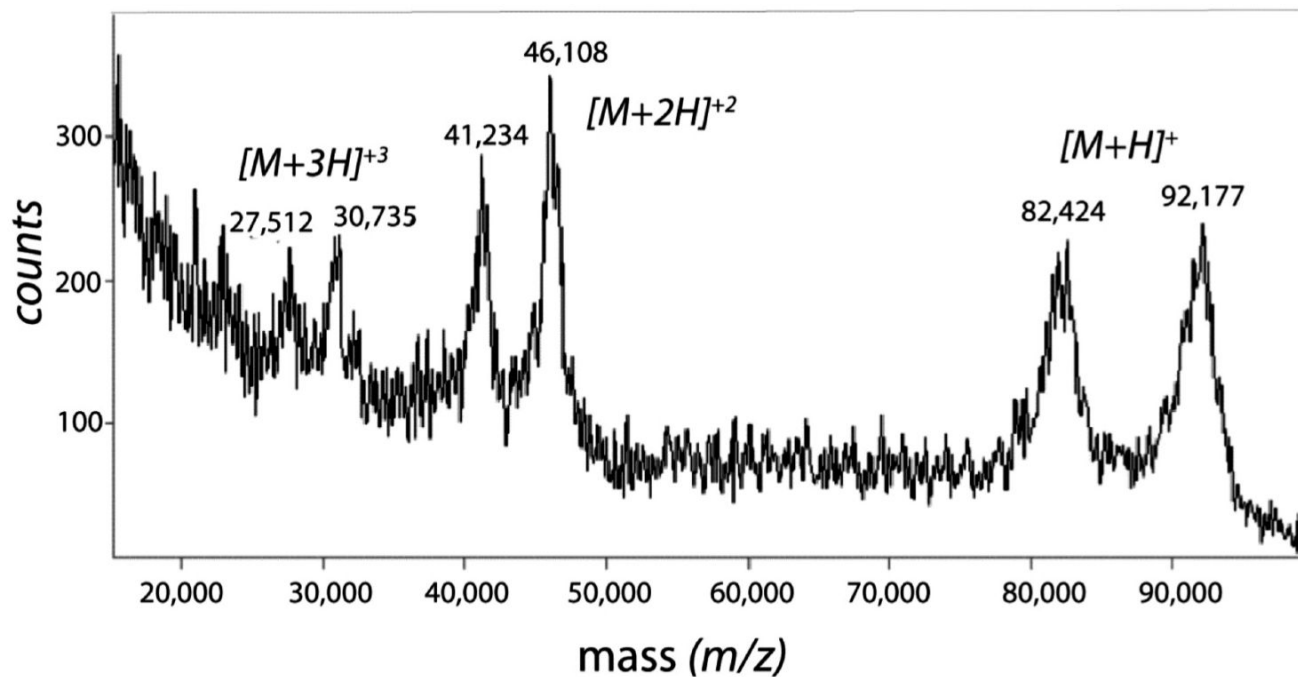
Figure 3.
MALDI-TOF mass spectrum of purified mcfp-1. Peak clusters from right to left are singly, doubly, and triply protonated ions. Operating parameters were delayed extraction (200 ns) in positive ion mode with accelerating voltage of 25000 V, grid voltage at 93%, and guide wire voltage at 0.1%. Spectrum represents the average of 254 scans.

¹ *MEGIKLNLCLLCIFSCDVFALSNG* ²⁴

²⁵ FIHNAYGSAYAGASAGAYKPLPGSYGSKHVPVY ⁵⁷
⁵⁸ KPMNKIPTSYISKKSYPAPYKPKGYHPTNSYQP ⁸⁰
⁹¹ TYGSKTNYPPIYKPVAKKLSSYKAIKTTYLVYK ¹²³

¹²⁴ AKTSYPPVYK HKITNPPTYK PKITYPPTYK PKPSYPPTYK PKPSYPPTYK ¹⁷³
¹⁷⁴ AKKTYPSTYK PKPSYPPTYK PKITYPPTYK PKPSYPPSYK AKKSYPSTYK ²²³
²²⁴ PKPSYPPTYK AKKTYPSTYK PKPSYPPTYK PKITYPPTYK PKPSYPPSYK ²⁷³
²⁷⁴ AKKSYPSTYK PKPSYPPTYK PKITYPPTYK PKPSYPPTYK AKKTYPPTYK ³²³
³²⁴ PKITYPPTYK PKPSYPTSYK SKKTYPPTYK PKITYPPTYK PKPSYPPSYK ³⁷³
³⁷⁴ PKITYPPTYK PKKSYPPAYK SKASYPPSYQ PKKTYLPSYK PKKTYPPTYK ⁴²³
⁴²⁴ RKISYPPTYK TKPSYPSSYK RKTSYPSTYK RKTSYPPTYK PKISYPSTYK ⁴⁷³
⁴⁷⁴ TKPSYPPTYK AKKTYPPTYK PKITYPPTYK PKPSYPTSYK SKKTYPPTYK ⁵²³
⁵²⁴ PKITYPPTYK PKPSYPPSYK PKITYPPTYK PKKSYPPAYK SKASYPPSYQ ⁵⁷³
⁵⁷⁴ PKKTYLPSYK PKKTYPPTYK RKISYPPTYK TKPSYPASYK RKTSYPSTYK ⁶²³
⁶²⁴ RKTSYPPTYK PKISYPSTYK TKPSYPPTYK PKPSYASSYK PKIRYPPTYK ⁶⁷³
⁶⁷⁴ PKPSYASSYK PKITYPPTYK PKISYPPTYK PKITYPPSYK PKISYLPAYK ⁷²³
⁷²⁴ PKISYPSQY ⁷³²

PKISYPPTYK ⟶ P*KISY*P**P*TY*K

Figure 4.
Complete sequence of mcfp-1 variant 1 deduced from cDNA. Signal peptide is denoted in italics, and partial sequences known from Edman sequencing and a partial cDNA are underlined with dashes. The cartoon below shows the domain structure consisting of a nonrepetitive N-terminus (NR) and the majority consisting of a decapeptide (consensus PKISYPPTYK) repeated 64 times in tandem. Known modifications in the mature protein are 4-Hyp (P*), 3, 4-diHyp (P**), and Dopa (Y*).

Mytilus species	Mfp1 variant	Mass$_{virt}$ kDa	Mass$_{obs}$ kDa	Consensus sequence	Repeat #	Ref
californianus	1	82.4	92.2	PKISYPPTYK	64	here
	2	75.5	82.4	"	58	here
coruscus	1	99.1	?	PKISYPPTYK	73	36
edulis	1	100.4*	108.6	AKPSYPPTYK AKPTYK	74 14	18
	2	101.9	108.6	AKPSYPPTYK AKPTYK	72 13	19 39
galloprovincialis	1	83.2	90.4	AKPSYPPTYK	65	21; supporting

Figure 5.
Comparison of mfp-1 variants in *Mytilus californianus* with related homologues in other *Mytilus* species. Comparison of virtual and observed masses, consensus peptide sequence, and repeat frequency in mfp-1 from four *Mytilus* species. Masses are average masses. The virtual mass for Mefp-1 variant 1 (100.4* kDa) is based on an incomplete genomic sequence, hence likely to be slightly larger.

Table 1

Amino Acid Composition of mfp- 1s from *M. californianus*, *M. galloprovincialis* (13), and *M. edulis* (19), respectively, in Mole % (res/100 res)[a]

amino acid	Mcfp-1		Mgfp-1		Mefp-1	
	actual	virtual	actual	virtual	actual	virtual
di-Hyp	5.9		4.1		3.0	
Hyp	18.2		10.7		10.2	
Asx	2.6	0.7	3.8	1.1	2.3	0.8
Thr	9.7	11.4	10.9	10.5	11.7	12.2
Ser	9.7	11.2	8.4	12.3	10.2	9.9
Glx	1.8	0.6	2.3	0.3	0.9	0.2
Pro	3.8	24.4	6.7	24.8	8.1	25.6
Gly	2.4	1.0	3.3	1.0	3.1	0.1
Ala	4.2	3.4	7.5	7.0	8.1	7.5
Cys	0	0	0.0	0.0	0.0	0.0
Val	1.3	0.7	1.7	0.5	0.8	0.5
Met	0	0.1	0	0.1	0.1	0.1
Ile	3.2	3.7	1.0	1.1	0.8	0.7
Leu	1.1	0.8	1.1	1.1	1.1	1.0
Dopa	13.0		10.6		10.5	
Tyr	5.8	19.4	7.2	19.6	6.6	19.2
Phe	0.4	0.1	0.4	0.1	0.1	0.0
His	0.4	0.6	0.6	0.4	0.8	0.2
Hyl	0.3		0.7		0.1	
Lys	19.4	20.9	19.6	19.6	21.1	21.7
Arg	1.0	1.0	1.2	0.5	0.7	0.2
total	100	100	100	100	100	100

[a] Actual represents measured composition after protein hydrolysis and amino acid analysis ($n = 3$, sd $\pm 15\%$), whereas virtual denotes composition calculated from the cDNA deduced sequences of mcfp-1 variant 1, mgfp-1, and mefp-1.